



Published in final edited form as:

*Semin Ophthalmol.* 2012 ; 27(0): 107–116. doi:10.3109/08820538.2012.707276.

## Confocal Microscopy of Corneal Dystrophies

Anita N. Shukla, Andrea Cruzat, and Pedram Hamrah

Ocular Surface Imaging Center, Cornea & Refractive Surgery Service, Massachusetts Eye & Ear Infirmary, Department of Ophthalmology, Harvard Medical School, Boston, MA, USA

### Abstract

*In vivo* confocal microscopy (IVCM) of the cornea is becoming an indispensable tool in the cellular study of corneal physiology and disease. This technique offers non-invasive imaging of the living cornea with images comparable to that of *ex vivo* histology. The ability to provide high-resolution images of all layers in the living cornea has resulted in new discoveries of corneal pathology at the cellular level. The IVCM analysis of corneal dystrophies is of importance to clinicians, as current methods of diagnosis involve slit-lamp characteristics, genetic analysis, and invasive biopsy. IVCM is helpful in evaluating the morphological characteristics of corneal dystrophies at the histological level and may be helpful in diagnosis, determination of progression, and understanding the pathophysiology of disease. The purpose of this review is to describe the principles, applications, and clinical correlation of IVCM in the study of corneal dystrophies.

### Keywords

Cornea; Dystrophy; Confocal microscopy

## INTRODUCTION

The term “corneal dystrophy” has been used to refer to a group of inherited corneal diseases that are typically bilateral, symmetric, and slowly progressive. Although the dystrophies can be classified according to severity, genetics, histopathology, or biochemical characteristics, the most commonly used classification system has been anatomically based.<sup>1</sup> The dystrophies are typically classified by level of the cornea that is involved, which separates these entities into epithelial and subepithelial, Bowman’s layer, anterior stromal, posterior stromal/ Descemet’s, and endothelial dystrophies.<sup>1</sup> Current methods of diagnosis involve slit-lamp characteristics, genetic analysis and invasive biopsy; however, *in vivo* confocal microscopy (IVCM) is rapidly becoming a useful method in evaluating the morphological characteristics of corneal dystrophies at the histological level.

Goldman first described a confocal slit system with line illumination in 1940. However, the confocal microscope was invented and patented by Minsky in 1957.<sup>2</sup> In 1968, the tandem scanning confocal microscope (TSCM) and later the slit scanning confocal microscope (SSCM) were developed, such as the Confoscan (Nidek Technologies, Italy). It was not until 1985 that confocal microscopy was used by Lemp et al. to examine the cornea.<sup>3</sup> A more recent improvement in this technology was the use of coherent light to produce the laser

© 2012 Informa Healthcare USA, Inc.

Correspondence: Pedram Hamrah, MD, Massachusetts Eye & Ear Infirmary, Cornea Service, 243 Charles Street, Boston, MA 02114, USA. pedram\_hamrah@meei.harvard.edu.

**Declaration of interest:** The authors report no conflicts of interest. The authors alone are responsible for content and writing of the paper.

scanning confocal microscope (LSCM) Heidelberg Retinal Tomograph 3 (HRT3) in conjunction with the Rostock Cornea Module (RCM) (Heidelberg Engineering, Germany), which uses a 670 nm wavelength diode laser. While conventional light microscopes are limited by light scatter from structures outside of the focal plane, confocal microscopes create a point source of light by a pinhole aperture, focused by an objective lens on the tissue. The light reflected by the specimen is then collected by a parallel objective lens, focused onto a separate pinhole aperture, and collected by a detector. The illuminating point source and the observation aperture of the detector are conjugate with the same point in the tissue, hence the term “confocal.”<sup>4</sup>

With a growing interest in non-invasive techniques to study live cellular physiology in both health and disease, the development and application of *in vivo* confocal microscopy (IVCM) has enabled ophthalmologists to make a quantum leap in the diagnosis and management of corneal disorders. Slices of the cornea can be examined individually, enabling detailed layer-by-layer observations, and the exact depth of findings can be identified.<sup>5</sup> Aside from the huge leap in advancing our understanding of corneal cellular and nerve morphology, the greatest utility of this technique has been the quantitative assessment of corneal cellular and nerve properties in normal health, disease, and postoperatively.<sup>6</sup> Investigators have described the relationship of cells, nerves, and deposits throughout the cornea, and related these to clinical and histopathological findings.<sup>7</sup> With the ease of clinical set-up, high throughput, and 800-fold magnification of live cellular architecture, IVCM holds profound promise towards enhancing the quality of care provided to patients in an out-patient setting. However, the lack of software available to perform automated analysis requires in-depth knowledge and training to accurately assess the quantitative and qualitative aspects of obtained images.

In this review, we illustrate the remarkable advances made to date by the use of IVCM to promote a better understanding of corneal dystrophies. The purpose of this review is to aid clinicians in the diagnosis of corneal dystrophies when the diagnosis is not obvious by slit-lamp biomicroscopy. IVCM is helpful in evaluating the morphological characteristics of corneal dystrophies at the histological level and may be helpful in diagnosis, determination of progression, and understanding the pathophysiology of disease. The ability to provide high-resolution images of all layers in the living cornea has resulted in new discoveries of corneal pathology at the cellular level.

## MATERIALS AND METHODS

Articles assessed for inclusion in this review were identified by a Medline search in August 2011 using keywords “cornea,” “dystrophy,” and “confocal.” The references section of the identified publications was also reviewed. Synthesis of the selected literature focused on the use of *in vivo* confocal microscopy for corneal dystrophies was included in this paper.

## RESULTS

### Epithelial and Subepithelial Corneal Dystrophies (Table 1)

**Epithelial Basement Membrane Dystrophy (EBMD)**, also called map-dot-fingerprint dystrophy and Cogan’s microcystic dystrophy, is the most common anterior corneal dystrophy and is associated with corneal epithelial erosions in about 10% of cases. The clinical components include gray epithelial patches with sharply demarcated edges (maps), clear or white microcysts (dots), gray or refractile fine lines (fingerprints), and the irregular smudgy changes of epithelial erosion.

IVCM reveals thin, highly reflective thickened linear tissue within the intermediate and basal epithelial cell layers and anterior stroma corresponding to abnormal basement membrane extending into the epithelium.<sup>8–11</sup> High-contrast, round, droplet-shaped cysts ranging in size between 10 and 400  $\mu\text{m}$  within the epithelium have been identified.<sup>8–10</sup> Basal epithelial cells around the abnormal basement membrane seem to be highly distorted with distended cytoplasm and very reflective nuclei.<sup>8–10</sup> Additionally, various pathologic findings in the subbasal nerve plexus with short or abnormally shaped nerve fiber bundles and decreased numbers of long-nerve fiber bundles have been described (Figure 1).<sup>11</sup>

**Meesmann Corneal Dystrophy (MECD)** is an autosomal dominant corneal dystrophy characterized by multiple tiny cysts or vacuoles in the epithelium. Histopathologically, the characteristic finding consists of small cysts in the epithelium, which are filled with periodic acid–Schiff–positive cellular debris. These represent an intracytoplasmic “peculiar substance” representing collection of fibrogranular material as shown by transmission electron microscopy.

IVCM demonstrates hyporeflexive, well-delineated areas in the basal epithelial layer corresponding to the multiple epithelial cystic lesions seen by slit-lamp bio-microscopy. The majority are circular, oval, or teardrop-shaped and range between 40 and 150  $\mu\text{m}$  in diameter. Reflective spots are visible within most of the lesions and may represent the fibrillogranular material (termed peculiar substance) observed by electron microscopy studies. A fragmented appearance of the subbasal nerve plexus has also been observed.<sup>12</sup> In contrast, IVCM of the cornea in EBMD demonstrates larger cystic lesions, which do not exhibit the hyperreflectivity within them as observed in Meesmann’s.<sup>12</sup>

**Lisch Epithelial Corneal Dystrophy (LECD)** is characterized as a band-shaped and whorled microcystic dystrophy of the corneal epithelium. A single case of LECD examined by IVCM has been reported describing many solitary dark and well-bounded lesions (50–100 nm) with round and oval configurations. Some lesions showed reflective points in the center corresponding to the cell nuclei. Between the dark lesions, innumerable crowded and well-bounded hyperreflective patches were noted.<sup>13</sup> There was involvement of all epithelial layers extending to the limbus.<sup>14</sup>

**Gelatinous Droplike Dystrophy (GDLD)** is a rare, autosomal recessive disease, characterized by the deposition of amyloid material in the subepithelial space of the cornea. Jing et al. investigated two brothers with GDLD. IVCM revealed an overall mild disorganization of the epithelial architecture with epithelial cells that were irregular in shape and often elongated. At the level of Bowman’s layer, only very small numbers of subbasal nerves with increased background intensity were detected. Large accumulations of brightly reflective amyloid material were noted within or beneath the epithelium and within the anterior stroma. Keratocyte nuclei were poorly identifiable and were embedded in the extracellular matrix with increased reflectivity.<sup>15</sup>

### **Bowman Layer Corneal Dystrophies (Table 2)**

**Reis-Bücklers Corneal Dystrophy (RBCD)** also known as corneal dystrophy of Bowman’s layer, type I, is a rare dystrophy. The Bowman’s layer undergoes disintegration and is replaced by a sheet-like connective tissue layer with granular Masson trichrome–red deposits. Transmission electron microscopy, necessary for definitive histopathologic diagnosis, demonstrates subepithelial, rod-shaped bodies. This disease has been associated with mutations in the TGFBI gene. Symmetrical reticular opacities, usually appearing bilaterally in the upper cornea by the age of four or five years, elevate the corneal epithelium, leading eventually to corneal erosions.

**Thiel-Behnke Corneal Dystrophy (TBCD)**, also known as corneal dystrophy of Bowman's layer, type II, is a rare autosomal dominant form of human corneal dystrophy affecting the Bowman's layer. Some cases are linked to chromosome 10q24; others stem from a mutation in the TGFBI gene. The honeycomb pattern of degenerative changes in the corneal epithelium and Bowman's membrane helps to distinguish this disorder from other anterior corneal dystrophies.

In both dystrophies, the Bowman's layer is completely replaced with pathologic material; however, reflectivity is much higher in RBCD than in TBCD. Kobayashi et al. compared two patients with RBCD and three patients with TBCD by IVCN. In Thiel-Behnke dystrophy, deposits in the epithelial basal cell layer showed homogeneous reflectivity with round-shaped edges accompanying dark shadows. In contrast, deposits in the same cell layer for patients with RBCD showed high reflectivity from small granular materials without shadows.<sup>16,17</sup> Werner et al. studied three patients with RBCD. Bowman's layer was generally absent and replaced by a highly reflective, irregular material as described by Kobayashi. The anterior stroma contained fine, diffuse deposits of dystrophic material interspersed between keratocyte nuclei (Figure 2).<sup>18</sup> It has been hypothesized that the basic alteration in this dystrophy is in the superficial keratocytes, which produce abnormal material that replaces Bowman's layer.<sup>19</sup>

### Anterior Stromal Dystrophies (Table 3)

**Schnyder's Crystalline Corneal Dystrophy (SCD)** is an autosomal dominant disease, characterized by corneal stromal cholesterol deposition in the anterior one-third of the stroma and Bowman's layer, accompanied by a diffuse, gray stromal haze. By IVCN, large accumulations of brightly reflective crystalline material, needle-shaped or rectangular, are found in the Bowman's layer and anterior to the mid-stroma with markedly decreased density of keratocytes.<sup>20–22</sup> The shape and numbers of crystalline deposits in the anterior stroma differ among patients despite quite similar clinical appearance.<sup>23</sup> The posterior stroma shows fine needle-shaped deposits within the matrix, decreasing in number and brightness with depth.<sup>21,24</sup> With time, the normal corneal architecture becomes disturbed by large intracellular and extracellular crystalline deposits and accumulation of highly reflective extracellular matrix, resulting in central opacity and disruption of the sub-epithelial nerve plexus. The nerve plexus presents with an irregular tortuous appearance.<sup>20,22</sup> Neural regeneration after keratectomy appears delayed in these cases.<sup>22</sup>

**Granular corneal dystrophy (GCD)**, an autosomal dominant disease, causes a loss of corneal transparency due to an accumulation of "bread-crumbs"-like hyaline deposits within the corneal stroma or Bowman's layer.<sup>25</sup> They typically involve the central cornea and a clear zone of unaffected tissue is found between the affected area and the limbus. Granular dystrophy, Avellino dystrophy, Reis-Bucklers dystrophy, and lattice dystrophy have all been found to be associated with mutations in the 5q31-related TGFBI gene (BIGH3).<sup>25</sup>

On IVCN, images of the epithelium and anterior stroma demonstrate central corneal irregularity.<sup>25</sup> Irregular, highly reflective breadcrumb deposits of 50  $\mu\text{m}$  in diameter are found between the intermediate epithelial cell layer and Bowman's layer.<sup>18</sup> Deposits in the stroma vary from round to irregular, trapezoidal-shaped and are between 50 to 500  $\mu\text{m}$  in diameter. The lesions generally are highly reflective, dense, gray-white, and separated by clear (dark) areas of normal stroma. Isolated smaller trapezoidal-shaped deposits, 30 to 50  $\mu\text{m}$  in diameter, occasionally were found in the deeper stroma surrounded by normal keratocytes. The deep stroma also contained multiple, highly reflective punctiform deposits, 5 to 10  $\mu\text{m}$  in diameter, interspersed with round structures, probably keratocyte nuclei.<sup>18</sup> Images from the superficial layers of the cornea showed flat deposits, while those in the

deeper layers had a more three-dimensional form.<sup>18</sup> Around the anterior stromal lesions, thin subbasal nerve fibers were clearly visible.<sup>5</sup>

**Lattice corneal dystrophy (LCD)** is characterized by Arg124Cys and Leu527Arg mutations of TGFBI.<sup>25</sup> Slit-lamp biomicroscopy shows numerous threadlike, radially oriented fine spicules throughout the stroma corresponding to amyloid deposits. Kaufman et al. first described a case of primary corneal amyloidosis and demonstrated the hyperreflective nature of amyloid deposition with confocal microscopy.<sup>26</sup> Since then, studies have described highly reflective punctiform extracellular deposits in the basal epithelial layer.<sup>18,27</sup> In the stroma, highly reflective linear filaments up to 50  $\mu\text{m}$  in diameter and thick branching filaments 80 to 100  $\mu\text{m}$  in diameter have been noted with changing reflectivity and poorly demarcated margins.<sup>18,27,28</sup> Changing reflectivity corresponds to the lack of homogeneity of deposits.<sup>28</sup> A reduction of long-nerve fiber bundles in the subbasal nerve plexus, which results in decreased mechanical and thermal sensitivity, has also been described in a case of lattice type II (Familial Amyloidosis).<sup>29</sup>

In **Macular corneal dystrophy (MCD)** (Ala217Thr mutation of the carbohydrate sulfotransferase gene [CHST6]), an autosomal recessive disease, slit-lamp biomicroscopy demonstrates ground glass-like haze with indistinct borders throughout the thickness of the cornea. Kobayashi et al. used IVCN to study two patients with macular dystrophy. They demonstrated homogeneous light reflective materials with dark striae-like images throughout the anterior stroma. Normal keratocytes were not seen.<sup>27</sup>

In **Avellino corneal dystrophy**, or combined granular-lattice corneal dystrophy (GCD2), (Arg124His mutation of human transforming growth factor-induced gene [TGFBI]), multiple, discrete, round, sharply demarcated gray-white deposits, as well as scattered stellate opacities are appreciated on slit-lamp microscopy.<sup>27</sup> By IVCN, focal deposition of highly reflective granular materials without dark shadows is observed in the basal epithelial layer. Clusters of highly reflective granular materials with irregular edges are observed at the level of the superficial and middle stroma. The surrounding stroma and keratocyte nuclei, as well as the endothelial layer, appear normal. Interestingly, lattice-like lesions were not appreciated in seven patients examined (Figure 3).<sup>27</sup> Because Avellino and RBCD have histological features of granular dystrophy, it is not surprising that they have similar laser confocal images. *In vivo* laser confocal microscopy is able to differentiate these histologically similar dystrophies because there is no apparent mid-stromal involvement in RBCD.

#### Posterior Stromal Dystrophies (Table 4)

Several corneal dystrophies such as Cornea Farinata, Punctate Dystrophy, Pre-Descemet's Dystrophy, Fleck's Corneal dystrophy, Deep Filiform Dystrophy, and Posterior Punctiform Dystrophy have the clinical appearance of fine opacities limited to the posterior corneal stroma.<sup>30</sup> IVCN has been useful in differentiating these cases and might aid with an improved classification for these entities.

**Cornea Farinata** is an asymptomatic degenerative condition characterized by a myriad of fine, dust-like opacities found bilaterally in the posterior stroma near Descemet's membrane. They are best seen on retro-illumination and appear grey-brown to white in color.<sup>30</sup> Kobayashi et al.<sup>31</sup> reported two cases with cornea farinata. Using IVCN, highly reflective small particles were observed in the cytoplasm of keratocytes in the deep stroma adjacent to the corneal endothelial layer. No abnormalities of the Descemet's membrane and endothelial cell layers were noted.

**Pre-Descemet's Corneal dystrophy (PDCD)**, a condition bearing a close clinical resemblance to Cornea Farinata, typically manifests in patients older than 30 years of age. On slit-lamp examination, larger and more polymorphous opacities than those of Cornea Farinata or Fleck's dystrophy are seen, distributed throughout the cornea but with a predilection for the deep stroma.<sup>32</sup> IVCN demonstrates intra- and extra-cellular hyper-reflective inclusions, pleomorphic in shape and size, measuring from 30  $\mu\text{m}$  to 80  $\mu\text{m}$  immediately anterior to Descemet's membrane and prominent subbasal nerves (Figure 4).<sup>30</sup> The intracellular particles have been noted inside enlarged keratocytes with abnormally visible intercellular processes. The pleomorphic structures may be the enlarged posterior keratocytes, and small inclusions may be secondary lysosomes containing lipofuscin-like lipoprotein.<sup>33</sup> Based on IVCN, the diagnosis of pre-Descemet's dystrophies should be limited to those dystrophies where IVCN rules out the involvement of the anterior and mid-stroma.<sup>30</sup>

**Fleck's Corneal Dystrophy (FCD)** is a rare auto-somal dominant corneal dystrophy with bilateral small gray-white fleck-like or wreath-like opacities scattered in all layers of the corneal stroma from the center to the periphery, with clear intervening stroma.<sup>34</sup> Histopathologically, relatively large cytoplasmic vacuoles containing excess glycosaminoglycan and lipids are found inside keratocytes throughout the stroma.<sup>5</sup>

Intracellular hyperreflective dots of various shapes throughout the corneal stroma have been reported on IVCN. These consist mostly of small spherical matter with a diameter of 1–18  $\mu\text{m}$ , which are sometimes enclosed in cyst-like structures and numerous large doughnut-like or nephroid-like particles, measuring 50–110  $\mu\text{m}$  in diameter in the mid- and posterior stroma.<sup>5,34,35</sup> Inclusions are restricted to intracellular compartments, unlike pre-Descemet's dystrophy where extracellular particles or particles within keratocyte processes are also observed.<sup>5,36</sup> The subbasal nerves show hyperreflective inclusions and the branch and density of the subbasal nerves is reduced, which may contribute to the decreased corneal sensitivity observed in Fleck's corneal dystrophy.<sup>37</sup>

**Central Cloudy Dystrophy of Francois (CCDF)** is a bilateral, symmetric stromal dystrophy with dense opacities centrally and posteriorly. Opacities are multiple, nebulous, polygonal, gray areas, separated by crack-like intervening zones. Vision is usually not reduced. Kobayashi et al. studied two patients with CCDF by IVCN and noted normal superficial and basal epithelial layers, mid-stromal layers, and endothelial layers. However, small highly refractile granules and deposits were observed in the anterior stromal layer in both cases. These granules might correspond to fibrillo-granular materials or localized aggregates of acid muco-polysaccharide beneath the basement membrane of the epithelium. Also, multiple dark striae among the extra-cellular matrix were observed in the posterior stroma adjacent to the corneal endothelial layer. The directions of these microstriae were highly variable, appearing as vertical, horizontal, oblique, or reticular lines.<sup>38</sup>

**Posterior Amorphous Corneal Dystrophy (PACD)** presents as diffuse gray-white, sheet-like opacities which occur in the deep stroma in the first decade of life. Corneal thinning to as low as 380  $\mu\text{m}$ , a flattened corneal topography (<41.00 D), and hyperopia are occasionally present.

Prominent Schwalbe's line, fine iris processes, pupillary remnants, iridocorneal adhesions, corectopia, pseudopolycoria, and anterior stromal tags have been reported.<sup>1</sup> Erdem et al. reported a single case of PACD in which IVCN demonstrated microfolds and diffuse hyper-reflective sheet-like opacities with spikes extending from the posterior stroma to the stroma immediately adjacent to the endothelial layer. The deposits appeared to be primarily extracellular.<sup>39</sup>

## Endothelial Dystrophies (Table 5)

**Fuchs' Endothelial Corneal Dystrophy (FECD)** is a bilateral, slowly progressing disease of the cornea characterized by a dysfunctional endothelial cell layer. Clinical findings vary with the severity of the endothelial disease, including an abnormal endothelial layer with cornea guttata, pigment dusting, and beaten metal appearance, Descemet's membrane thickening, stromal edema, subepithelial fibrosis, epithelial edema, and bullae. The endothelial cells are noted to be larger and more polymorphic and are disrupted by excrescences of excess collagen.<sup>32</sup>

IVCM reveals the presence of round hyporeflexive images in large size and number, with an occasional central highlight at the level of the endothelium.<sup>32,40–43</sup> Between them, pleomorphic and polymegathic endothelial cells appeared hyperreflective and could not be identified individually. In the late stage, diffuse hyporeflexive areas surrounded by hyperreflective endothelial cells were noted. Within the corneal stroma, the collagen fibers were blurred and the background illumination was increased secondary to edema in the anterior stroma. Qualitative examination confirmed a sparse population of keratocytes in the anterior stroma.<sup>44</sup> Lacunae and 5–20  $\mu\text{m}$  wide dark bands against increased background reflection were noted in the posterior stroma. The dark bands may represent folds of Descemet's membrane, collagen lamellae separated by edema, or pockets of fluid. Descemet's membrane was thickened in all eyes.<sup>45,46</sup> A majority of eyes had absence of the subbasal nerve plexus (Figure 5).<sup>46</sup> Grupscheva et al.<sup>47</sup> used IVCM to differentiate corneal diseases that exhibit corneal edema and decreased transparency. They demonstrated that confocal microscopy may confirm the diagnosis of cornea guttata and Fuchs' corneal endothelial dystrophy by demonstrating the presence of guttae. Most importantly, they highlighted the importance of IVCM in cases of corneal edema, where specular microscopy may fail to visualize the endothelium.

**Posterior Polymorphous Corneal Dystrophy (PPCD)** should be included in the differential diagnosis of FECD, as it is also a primary dystrophy of the corneal endothelium. Biomicroscopic findings include grayish plaques, linear streaks, and vesicular lesions on the endothelial surface. IVCM has revealed craters, streaks, and cracks over the corneal endothelium surface.<sup>32,48</sup> Vesicular lesions appear as rounded dark areas with some cell detail apparent in the middle, giving a doughnut-like appearance. Railroad track lesions appear as band-like dark areas with irregular edges enclosing some smaller lighter cells resembling epithelium-like cells.<sup>1,48</sup>

Chiou et al. reported two patients with PPCD. At the level of Descemet's membrane, roundish hyporeflexive images were found in one patient. In the other patient, hyporeflexive bands were detected. In both patients, patchy hyperreflective areas were identified (Figure 6).<sup>49</sup>

## DISCUSSION

*In vivo* laser confocal microscopy is capable of high-resolution visualization of characteristic corneal microstructural changes, related to genetically mapped corneal dystrophies. The use of laser IVCM may be valuable in the differential diagnosis of corneal dystrophies, especially when diagnosis is otherwise uncertain, as observations obtained using IVCM are unique to each dystrophy. This modality is a useful technique to differentiate corneal dystrophies *in vivo*, bypassing the dependence on genetic studies and histopathology. IVCM may further be helpful in determination of progression, and understanding the pathophysiology of disease.

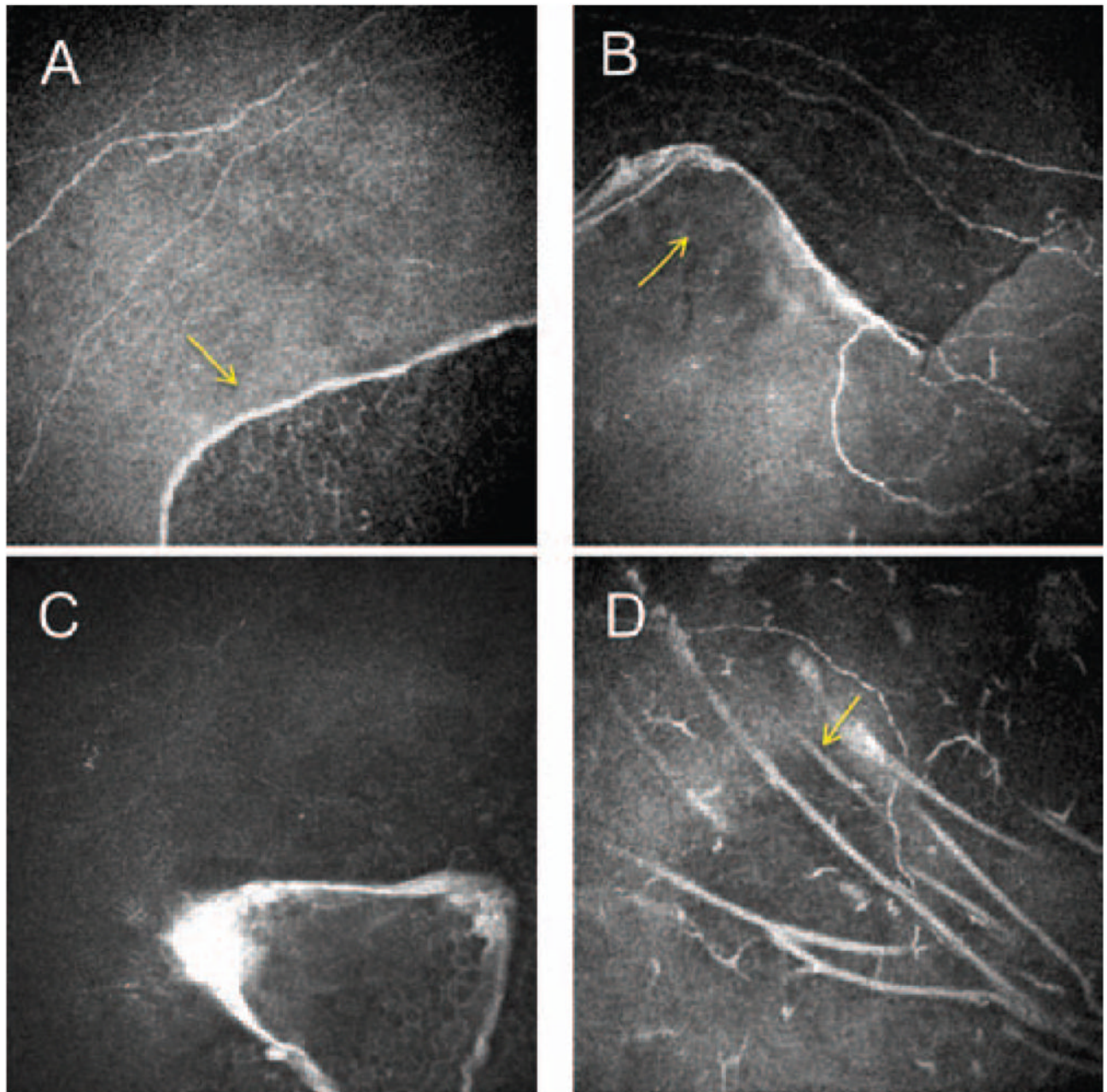
## References

1. Weiss JS, Moller HU, Lisch W, et al. The IC3D classification of the corneal dystrophies. *Cornea*. 2008; 27 (Suppl 2):S1–83. [PubMed: 19337156]
2. Patel DV, McGhee CN. Contemporary in vivo confocal microscopy of the living human cornea using white light and laser scanning techniques: A major review. *Clin Experiment Ophthalmol*. 2007; 35:71–88. [PubMed: 17300580]
3. Lemp MA, Dilly PN, Boyde A. Tandem-scanning (confocal) microscopy of the full-thickness cornea. *Cornea*. 1985; 4:205–9. [PubMed: 3836030]
4. Bochert R, Zhivov A, Kraak R, Stave J, Guthoff RF. Contribution to comprehension of image formation in confocal microscopy of cornea with Rostock cornea module. *Br J Ophthalmol*. 2005; 89:1351–5. [PubMed: 16170131]
5. Traversi C, Martone G, Malandrini A, Tosi GM, Caporossi A. In vivo confocal microscopy in recurrent granular dystrophy in corneal graft after penetrating keratoplasty. *Clin Experiment Ophthalmol*. 2006; 34:808–10. [PubMed: 17073913]
6. Erie JC, McLaren JW, Patel SV. Confocal microscopy in ophthalmology. *Am J Ophthalmol*. 2009; 148:639–46. [PubMed: 19674730]
7. Niederer RL, McGhee CN. Clinical in vivo confocal microscopy of the human cornea in health and disease. *Prog Retin Eye Res*. 2010; 29:30–58. [PubMed: 19944182]
8. Bozkurt B, Irkek M. In vivo laser confocal microscopic findings in patients with epithelial basement membrane dystrophy. *Eur J Ophthalmol*. 2009; 19:348–54. [PubMed: 19396777]
9. Hernández-Quintela E, Mayer F, Dighiero P, et al. Confocal microscopy of cystic disorders of the corneal epithelium 11 The authors have no commercial interest in the development or marketing of any products referred to in this article. *Ophthalmology*. 1998; 105:631–6. [PubMed: 9544636]
10. Labbe A, Nicola RD, Dupas B, Auclin F, Baudouin C. Epithelial basement membrane dystrophy: Evaluation with the HRT II Rostock Cornea Module. *Ophthalmology*. 2006; 113:1301–8. [PubMed: 16877069]
11. Rosenberg ME, Tervo TM, Petroll WM, Vesaluoma MH. In vivo confocal microscopy of patients with corneal recurrent erosion syndrome or epithelial basement membrane dystrophy. *Ophthalmology*. 2000; 107:565–73. [PubMed: 10711897]
12. Patel DV, Grupcheva CN, McGhee CN. Imaging the microstructural abnormalities of meesmann corneal dystrophy by in vivo confocal microscopy. *Cornea*. 2005; 24:669–73. [PubMed: 16015084]
13. Lisch W, Wasielica-Poslednik J, Lisch C, Saikia P, Pitz S. Contact lens-induced regression of Lisch epithelial corneal dystrophy. *Cornea*. 2010; 29:342–5. [PubMed: 20118787]
14. Kurbanyan K, Sejal KD, Aldave AJ, Deng SX. In vivo confocal microscopic findings in Lisch corneal dystrophy. *Cornea*. 2012; 31:437–41. [PubMed: 22222997]
15. Jing Y, Liu C, Wang L. A novel TACSTD2 mutation identified in two Chinese brothers with gelatinous drop-like corneal dystrophy. *Mol Vis*. 2009; 15:1580–8. [PubMed: 19693293]
16. Kobayashi A, Sakurai M, Shirao Y, Sugiyama K, Ohta T, Amaya-Ohkura Y. In vivo confocal microscopy and genotyping of a family with Thiel-Behnke (honeycomb) corneal dystrophy. *Arch Ophthalmol*. 2003; 121:1498–9. [PubMed: 14557196]
17. Kobayashi A, Sugiyama K. In vivo laser confocal microscopy findings for Bowman's layer dystrophies (Thiel-Behnke and Reis-Bucklers corneal dystrophies). *Ophthalmology*. 2007; 114:69–75. [PubMed: 17198850]
18. Werner LP, Werner L, Dighiero P, Legeais JM, Renard G. Confocal microscopy in Bowman and stromal corneal dystrophies. *Ophthalmology*. 1999; 106:1697–704. [PubMed: 10485537]
19. Akiya S, Brown SI. The ultrastructure of Reis-Bucklers' dystrophy. *Am J Ophthalmol*. 1971; 72:549–54. [PubMed: 4105521]
20. Ciancaglini M, Carpineto P, Doronzo E, Nubile M, Zuppari E, Mastropasqua L. Morphological evaluation of Schnyder's central crystalline dystrophy by confocal microscopy before and after phototherapeutic keratectomy. *J Cataract Refract Surg*. 2001; 27:1892–5. [PubMed: 11709268]

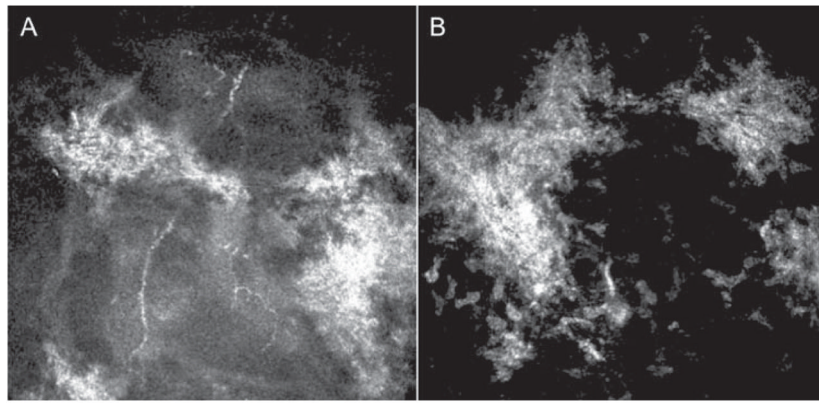


21. Jing Y, Wang L. Morphological evaluation of Schnyder's crystalline corneal dystrophy by laser scanning confocal microscopy and Fourier-domain optical coherence tomography. *Clinical & Experimental Ophthalmology*. 2009; 37:308–12. [PubMed: 19459870]
22. Vesaluoma MH, Linna TU, Sankila EM, Weiss JS, Tervo TM. In vivo confocal microscopy of a family with Schnyder crystalline corneal dystrophy. *Ophthalmology*. 1999; 106:944–51. [PubMed: 10328394]
23. Kobayashi A, Fujiki K, Murakami A, Sugiyama K. In vivo laser confocal microscopy findings and mutational analysis for Schnyder's crystalline corneal dystrophy. *Ophthalmology*. 2009; 116:1029–37. e1. [PubMed: 19394700]
24. Jing Y, Liu C, Xu J, Wang L. A novel UBIAD1 mutation identified in a Chinese family with Schnyder crystalline corneal dystrophy. *Mol Vis*. 2009; 15:1463–9. [PubMed: 19649163]
25. Dalton K, Schneider S, Sorbara L, Jones L. Confocal microscopy and optical coherence tomography imaging of hereditary granular dystrophy. *Cont Lens Anterior Eye*. 2010; 33:33–40. [PubMed: 19945908]
26. Kaufman SC, Beuerman RW, Goldberg D. A new form of primary, localized, corneal amyloidosis: A case report with confocal microscopy. *Metab Pediatr Syst Ophthalmol*. 1995; 18:1–4. [PubMed: 9064489]
27. Kobayashi A, Fujiki K, Fujimaki T, Murakami A, Sugiyama K. In vivo laser confocal microscopic findings of corneal stromal dystrophies. *Arch Ophthalmol*. 2007; 125:1168–73. [PubMed: 17846354]
28. Chiou AG, Beuerman RW, Kaufman SC, Kaufman HE. Confocal microscopy in lattice corneal dystrophy. *Graefes Arch Clin Exp Ophthalmol*. 1999; 237:697–701. [PubMed: 10459621]
29. Rosenberg ME, Tervo TM, Gallar J, et al. Corneal morphology and sensitivity in lattice dystrophy type II (familial amyloid-dosis, Finnish type). *Invest Ophthalmol Vis Sci*. 2001; 42:634–41. [PubMed: 11222521]
30. Lanza M, Borrelli M, Benusiglio E, Rosa N. In vivo confocal microscopy of an apparent deep stroma corneal dystrophy: A case report. *Cases Journal*. 2009; 2:9317. [PubMed: 20062640]
31. Kobayashi A, Ohkubo S, Tagawa S, Uchiyama K, Sugiyama K. In vivo confocal microscopy in the patients with cornea farinata. *Cornea*. 2003; 22:578–81. [PubMed: 12883356]
32. Yeh SI, Liu TS, Ho CC, Cheng HC. In vivo confocal microscopy of combined pre-descemet membrane corneal dystrophy and fuchs endothelial dystrophy. *Cornea*. 2011; 30:222–4. [PubMed: 20847662]
33. Ye YF, Yao YF, Zhou P, Pan F. In vivo confocal microscopy of pre-Descemet's membrane corneal dystrophy. *Clin Experiment Ophthalmol*. 2006; 34:614–6. [PubMed: 16925715]
34. Pan F, Yao YF, Nie X, Zhang B. Clinical characteristics and in vivo confocal microscopic imaging of Fleck corneal dystrophy. *Zhejiang Da Xue Xue Bao Yi Xue Ban*. 2011; 40:321–6. [PubMed: 21671495]
35. Grupcheva CN, Malik TY, Craig JP, Sherwin T, McGhee CN. Microstructural assessment of rare corneal dystrophies using real-time in vivo confocal microscopy. *Clin Experiment Ophthalmol*. 2001; 29:281–5. [PubMed: 11720152]
36. Linke S, Bartsch U, Richard G, Klemm M. In vivo confocal microscopy of pre-endothelial deposits. *Graefes Arch Clin Exp Ophthalmol*. 2007; 245:309–12. [PubMed: 16550401]
37. Frueh BE, Bohnke M. In vivo confocal microscopy of fleck dystrophy. *Cornea*. 1999; 18:658–60. [PubMed: 10571294]
38. Kobayashi A, Sugiyama K, Huang AJ. In vivo confocal microscopy in patients with central cloudy dystrophy of Francois. *Arch Ophthalmol*. 2004; 122:1676–9. [PubMed: 15534129]
39. Erdem U, Muftuoglu O, Hurmeric V. In vivo confocal microscopy findings in a patient with posterior amorphous corneal dystrophy. *Clin Experiment Ophthalmol*. 2007; 35:99–102. [PubMed: 17300585]
40. Chiou AG, Kaufman SC, Beuerman RW, Ohta T, Soliman H, Kaufman HE. Confocal microscopy in cornea guttata and Fuchs' endothelial dystrophy. *Br J Ophthalmol*. 1999; 83:185–9. [PubMed: 10396196]
41. Kaufman SC, Beuerman RW, Kaufman HE. Diagnosis of advanced Fuchs' endothelial dystrophy with the confocal microscope. *Am J Ophthalmol*. 1993; 116:652–3. [PubMed: 8238235]

42. Dong WL, Zou LH, Pan ZQ, Wang L. Morphologic characteristics of cornea in Fuchs endothelial dystrophy observed by confocal microscopy. *Zhonghua Yan Ke Za Zhi*. 2004; 40:465–70. [PubMed: 15454061]
43. Patel DV, Phua YS, McGhee CN. Clinical and microstructural analysis of patients with hyper-reflective corneal endothelial nuclei imaged by in vivo confocal microscopy. *Exp Eye Res*. 2006; 82:682–7. [PubMed: 16359661]
44. Hecker LA, McLaren JW, Bachman LA, Patel SV. Anterior keratocyte depletion in Fuchs endothelial dystrophy. *Archives of Ophthalmology*. 2011; 129:555–61. [PubMed: 21220622]
45. Rokita-Wala I, Mrukwa-Kominek E, Gierek-Ciaciura S. Changes in corneal structure observed with confocal microscopy during Fuchs endothelial dystrophy. *Klin Oczna*. 2000; 102:339–44. [PubMed: 11286109]
46. Mustonen RK, McDonald MB, Srivannaboon S, Tan AL, Doubrava MW, Kim CK. In vivo confocal microscopy of Fuchs' endothelial dystrophy. *Cornea*. 1998; 17:493–503. [PubMed: 9756443]
47. Grupcheva CN, Craig JP, Sherwin T, McGhee CN. Differential diagnosis of corneal oedema assisted by in vivo confocal microscopy. *Clin Experiment Ophthalmol*. 2001; 29:133–7. [PubMed: 11446452]
48. Patel DV, Grupcheva CN, McGhee CN. In vivo confocal microscopy of posterior polymorphous dystrophy. *Cornea*. 2005; 24:550–4. [PubMed: 15968159]
49. Chiou AG, Kaufman SC, Beuerman RW, Maitchouk D, Kaufman HE. Confocal microscopy in posterior polymorphous corneal dystrophy. *Ophthalmologica*. 1999; 213:211–3. [PubMed: 10420102]



**FIGURE 1.** Laser confocal microscopic findings of patients with map-dot-fingerprint dystrophy. A–D. Subbasal nerve plexus and basal epithelial membrane alterations. Arrows show highly reflective thickened linear tissue within the intermediate and basal epithelial cell layers corresponding to abnormal basement membrane extending into the epithelium.

**FIGURE 2.**

Laser confocal microscopic findings of patients with Reis Buckler dystrophy. A. Bowman's layer is replaced by highly reflective, diffuse granular irregular material and decreased sub-basal nerve plexus. B. The anterior stroma contains fine, diffuse deposits of dystrophic material interspersed between keratocyte nuclei.

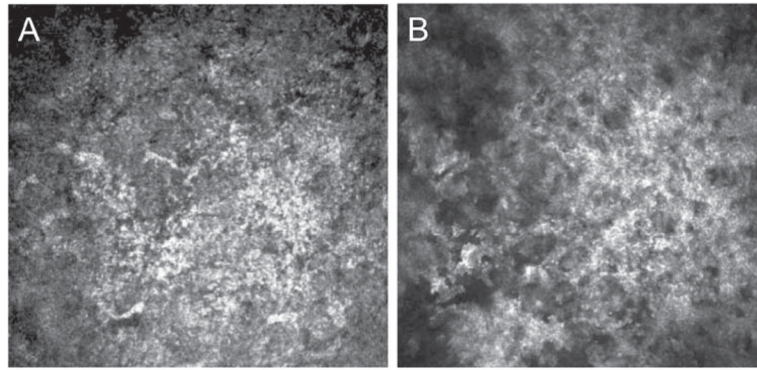


**FIGURE 3.** Laser confocal microscopic findings in a patient with Avellino dystrophy. A–B. Highly reflective granular material with irregular edges are observed at the level of the superficial and middle stroma.

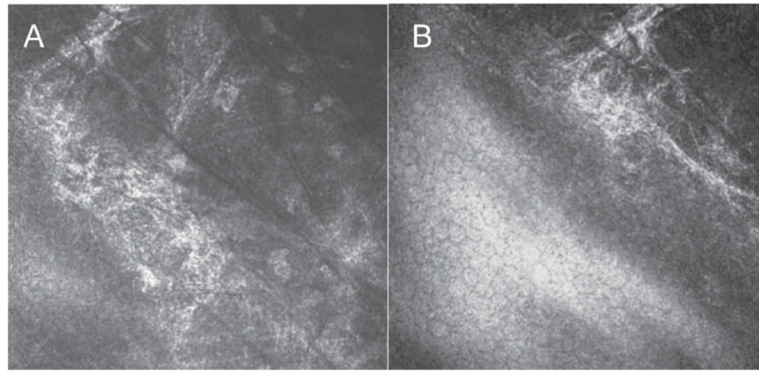


**FIGURE 4.** Laser confocal microscopic findings of patients with Pre-Descemet's dystrophy. A. Hyperreflective deposits in the deep stroma immediately anterior to Descemet's membrane. B. There is no involvement of the endothelial cell layer.

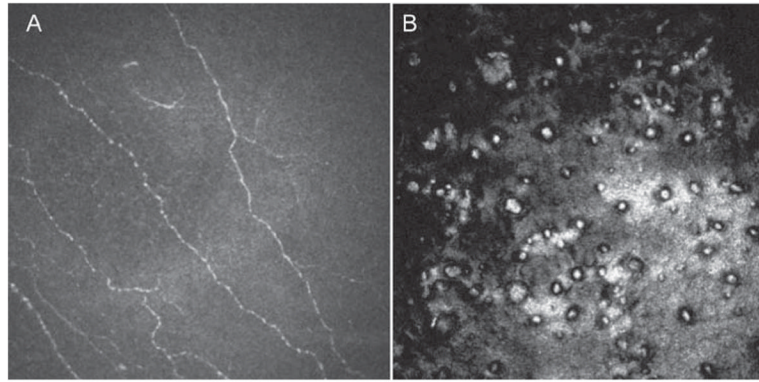


**FIGURE 5.** Laser confocal microscopic findings of patients with Fuchs dystrophy. A. Diminished corneal subbasal nerve plexus. B. Round hyporeflective images in different size and number with central highlight at the level of the endothelium.

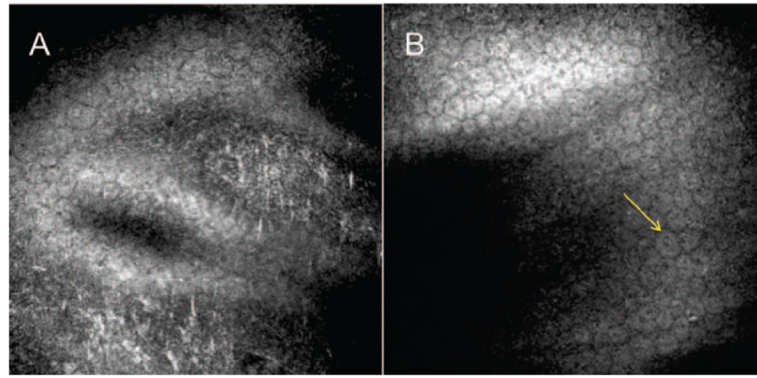


**FIGURE 6.** Laser confocal microscopic findings of patients with Posterior Polymorphous Corneal Dystrophy. A. At the level of Descemet's membrane, areas of hyperreflective lines and granules are identified. B. The corneal endothelial cell layer contains scattered endothelial cells with craters (arrow).



TABLE 1

## Epithelial and Subepithelial Corneal Dystrophies.

| Epithelial Dystrophies                        | IVCM Findings  | Reference / Number of Patients         | Type of IVCM         |
|---|--|--|----------------------|
| Epithelial basement membrane dystrophy (EBMD) | – Highly reflective linear tissue within the intermediate and basal epithelial cell layers and anterior stroma <sup>8-11</sup> | (8) Bozkurt et al./29                  | (8) Laser Scanning   |
|   | – 10–400 μm cysts within the epithelium <sup>8-10</sup>  | (9) Hernández-Quintela et al. /5       | (9) Scanning Slit    |
|   | – Highly distorted basal epithelial cells with distended cytoplasm and reflective nuclei. <sup>8-10</sup>                      | (10) Labbe et al./22                   | (10) Laser Scanning  |
|   | – Abnormal subbasal nerve plexus <sup>11</sup>   | (11) Rosenberg et al./8                | (11) Tandem Scanning |
| Meesmann corneal dystrophy (MECD)             | – Hyporeflective areas in the basal epithelial layer 10–145 μm in diameter <sup>12</sup>                                       | (12) Patel, Grupcheva, McGhee et al./3 | (12) Scanning Slit   |
|   | – Reflective spots visible within most of the lesions <sup>12</sup>  |  |                      |
|   | – Fragmented appearance of subbasal nerve plexus <sup>12</sup>   |  |                      |
| Lisch epithelial corneal dystrophy (LECD)     | – Solitary dark and well-bounded lesions (50–100 nm) with round and oval configurations <sup>13</sup>                          | (13) Lisch et al./1                    | (13) Laser Scanning  |
|   | – Hyperreflective epithelial cytoplasm with hyporeflective nuclei <sup>14</sup>  | (14) Kurbanyan et al./2                | (14) Laser Scanning  |
|   | – Innumerable crowded and well-bounded hyperreflective patches <sup>13</sup>   |  |                      |
| Gelatinous droplike dystrophy (GDL D)         | – Irregular and elongated epithelial cells <sup>14</sup>   | (14) Jing et al./1                     | (14) Laser Scanning  |
|   | – Decreased number of sub-basal nerves <sup>14</sup>   |  |                      |
|   | – Brightly reflective amyloid material within or beneath the epithelium and anterior stroma <sup>14</sup>                      |  |                      |

**TABLE 2**

## Bowman's Layer Corneal Dystrophies.

| <b>Bowman's Layer Corneal Dystrophies</b> | <b>IVCM Findings</b>  | <b>Reference / Number of Patients</b> | <b>Type of IVCM</b> |
|---|---|---------------------------------------|---------------------|
| Reis-Bucklers corneal dystrophy (RBCD)    | – Bowman's layer replaced by highly reflective granular material without shadows <sup>16</sup>                    | (16) Kobayashi, Sugiyama et al./ 3    | (16) Laser Scanning |
|   | – Anterior stroma with dystrophic material between keratocytes <sup>17</sup>                                      | (17) Werner et al./ 3                 | (17) Scanning Slit  |
| Thiel-Behnke dystrophy (TBCD)             | – Reflective epithelial basal cell layer deposits with round-shaped edges accompanying dark shadows <sup>16</sup> | (16) Kobayashi, Sugiyama et al./ 2    | (16) Laser Scanning |

TABLE 3

## Anterior Stromal Dystrophies.

| Anterior Stromal Dystrophies   | IVCM Findings   | Reference / Number of Patients   | Type of IVCM  |
|--|---|--|---|
| Schnyder's crystalline corneal dystrophy (SCD)                           | – Needle-shaped or rectangular reflective crystalline material, in Bowman's and anterior to mid-stroma & decreased keratocytes <sup>19-22</sup>   | (19) Ciancaglini et al./1<br>(20) Jing, Wang et al./ 1<br>(21) Vesaluoma et al./ 4 | (19) Scanning Slit<br>(20) Laser Scanning<br>(21) Tandem Scanning |
|  | – Fine needle-shaped deposits within the posterior stroma, decreasing in number with depth <sup>20,23</sup>   | (22) Kobayashi, Fujiki et al./ 6   | (22) Laser Scanning<br>(23) Laser Scanning                        |
|  | – Irregular, tortuous sub-basal nerve plexus <sup>19,21</sup>   | (23) Jing, Liu et al./2  |   |
| Granular corneal dystrophy (GCD)   | – 50 $\mu\text{m}$ reflective breadcrumb deposits between epithelial & Bowman's layer <sup>17,24</sup>  | (17) Werner et al./ 12   | (5) Laser Scanning<br>(17) Scanning Slit                          |
|  | – 50–500 $\mu\text{m}$ reflective round to irregular deposits in the anterior stroma <sup>17</sup>  | (24) Dalton et al./ 2  | (24) Scanning Slit  |
|  | – 30–50 $\mu\text{m}$ trapezoidal-shaped deposits and 5–10 $\mu\text{m}$ punctiform deposits interspersed with round keratocyte nuclei in deep stroma <sup>17</sup>                                   |  |   |
| Lattice corneal dystrophy (LCD)  | – Thin subbasal nerve fibers <sup>5</sup>   | (5) Travesi et al./ 2  |   |
|  | – Reflective punctiform extracellular deposits in the basal epithelial layer <sup>17,26</sup>   | (17) Werner et al./ 12<br>(26) Kobayashi, Fujiki et al./ 2                         | (17) Scanning Slit<br>(26) Laser Scanning                         |
|  | – Reflective linear filaments up to 50 $\mu\text{m}$ and thick branching filaments 80 to 100 $\mu\text{m}$ in the stroma with changing reflectivity and poorly demarcated margins <sup>17,26,27</sup> | (27) Chiou et al./ 2<br>(28) Rosenberg et al./ 20                                  | (27) Tandem Scanning<br>(28) Tandem Scanning                      |
| – Decreased long-nerve fiber bundles in the subbasal nerve <sup>28</sup> |   |  |   |
| Macular corneal dystrophy (MCD)  | – Homogeneous reflective materials with dark striae throughout the stroma. Normal keratocytes are not seen <sup>26</sup>  | (26) Kobayashi, Fujiki et al./ 2   | (26) Laser Scanning   |
| Avellino corneal dystrophy (GCD2)  | – Focal deposition of reflective granular material without dark shadows in the basal epithelial layer <sup>26</sup>   | (26) Kobayashi, Fujiki et al./ 7   | (26) Laser Scanning   |
|  | – Clusters of reflective granular material with irregular edges in superficial and middle stroma. <sup>26</sup>   |  |   |
|  | – Lattice lines are not discernible <sup>26</sup>   |  |   |

TABLE 4

## Posterior Stromal Dystrophies.

| Posterior Stromal Dystrophies                | IVCM Findings   | Reference / Number of Patients   | Type of IVCM   |
|--|---|--|--|
| Cornea Farinata                              | – Highly reflective small particles in the cytoplasm of keratocytes in the deep stroma adjacent to the corneal endothelial layer <sup>30</sup>  | (30) Kobayashi, Ohkubo et al./ 2   | (30) Scanning Slit   |
| Pre-Descemet's dystrophy (PDCD)              | – Intra- and extra-cellular hyperreflective inclusions pleomorphic in shape, 30 to 80 $\mu\text{m}$ in size immediately anterior to Descemet's membrane and prominent sub-basal nerves <sup>29</sup><br><br>– Intracellular particles inside enlarged keratocytes with abnormally visible intercellular processes. <sup>32</sup><br><br>– No involvement of the anterior and mid-stroma <sup>29</sup> | (29) Lanza et al./1<br>(32) Ye et al./ 1   | (29) Scanning Slit<br>(32) Scanning Slit   |
| Fleck's dystrophy (FCD)                      | – Intracellular reflective spherical matter 1–18 $\mu\text{m}$ enclosed in cyst-like structures and large 50–110 $\mu\text{m}$ doughnut-like particles in the mid- and posterior stroma <sup>5,33,34</sup><br><br>– Basal nerves with hyperreflective inclusions and reduced sub-basal nerves <sup>36</sup>   | (5) Travesi et al./ 2<br>(33) Pan et al./ 9<br>(34) Grupscheva et al./ 1<br><br>(36) Frueh et al./ 3 | (5) Laser Scanning<br>(33) Scanning Slit<br>(34) Scanning Slit<br>(36) Scanning Slit |
| Central cloudy dystrophy of Francois (CCDF)  | – Multiple dark striae in the posterior stroma adjacent to the endothelium appearing as vertical, horizontal, oblique, or reticular lines <sup>37</sup>   | (37) Kobayashi, Sugiyama et al./ 2   | (37) Scanning Slit   |
| Posterior amorphous corneal dystrophy (PACD) | – Microfolds and diffuse hyperreflective sheet-like extracellular opacities with spikes in the deep posterior stroma. <sup>38</sup>   | (38) Erdem et al./ 1   | (38) Scanning Slit   |

TABLE 5

## Endothelial Dystrophies.

| Endothelial Dystrophies                     | IVCM Findings   | Reference / Number of Patients                                 | Type of IVCM         |
|---|---|--|----------------------|
| Fuchs' endothelial corneal dystrophy (FECD) | – Large round hyporeflective images with occasional central highlight at endothelium <sup>31, 39, 41</sup>  | (31) Yeh et al./ 1<br>(39) Chiou, Kaufman et al./ 1            | (31) Scanning Slit   |
|   | – Hyperreflective pleomorphic and polymegathic endothelial cells which cannot be identified individually <sup>43</sup>  | (41) Dong et al./ 19   | (39) Tandem Scanning |
|   | – Stroma with blurred collagen fibers and increased background illumination <sup>43</sup>   | (43) Hecker et al./ 10<br>(44) Rokita-Wala et al./ 21          | (41) Scanning Slit   |
|   | – Sparse population of keratocytes in the anterior stroma <sup>43</sup>   | (45) Mustonen et al./ 11                                       | (43) Tandem Scanning |
|   | – Lacunae and 5–20 µm wide dark bands against increased back- ground reflection in posterior stroma <sup>44, 45</sup>   |  | (44) Scanning Slit   |
|   | – Thickened Descemet's <sup>44, 45</sup>  |  |                      |
| Posterior                                   | – Absent subbasal nerve plexus <sup>45</sup>  |  | (45) Scanning Slit   |
|   | – Endothelial surface with craters, streaks, and cracks <sup>31, 47</sup>   | (31) Yeh et al.  | (31) Scanning Slit   |
| Polymorphous Corneal Dystrophy (PPCD)       | – Vesicular lesions, rounded dark areas with doughnut-like appearance <sup>47</sup> - Railroad track lesions - band-like dark areas enclosing smaller lighter cells resembling epithelium <sup>47</sup> | (47) Patel, Grupcheva et al./ 6 (48) Chiou, Kaufman, et al./ 2 | (47) Scanning Slit   |
|   | – Descemet's with patchy hyperreflective areas and hyporeflective round images and bands <sup>48</sup>  |  | (48) Tandem Scanning |